Theor Chem Acc (2001) 106:223–232
DOI 10.1007/s002140100268

Theoretical
Chemistry Accounts

Regular article

A quantitative measure of bond polarity from the electron localization function and the theory of atoms in molecules

Stephan Raub, Georg Jansen

Institut für Theoretische Chemie, Heinrich-Heine-Universität Düsseldorf, Universitätsstraße 1 40225 Düsseldorf, Germany

Received: 10 January 2001 / Accepted 12 February 2001 / Published online: 22 May 2001

Abstract. A quantitative measure of the polarity of a bond can be obtained through combining the two complementary topological partitionings of the electron density obtained from the atoms in molecules theory, on the one hand, and the electron localization function, on the other. This requires an integration of the electron density in the atomic subbasins of a common bond electron localization basin. We present the first numerical application of the resulting topological definition of bond polarity to a set of small linear systems consisting of the FCN, HF, HCl, HBr, and NaCl molecules and the NeAr van der Waals dimer. It is shown that the findings are essentially in line with common expectation for these simple molecules, thus confirming the potential value of the novel bond polarity index for the analysis of controversial bonding situations. Additional insight is provided through the detailed investigation of fluctuations in the basin populations.

Key words: Electron localization function – Atoms in molecules – Bond polarity – Ionic character – Electronegativity

1 Introduction

The notion of the polarity of a bond is central to a large part of a chemist's qualitative understanding of the electronic structure of molecules [1, 2]. It is intimately connected with the concept of electronegativity, which according to Pauli [3, 4] can be defined as "the power of an atom in a molecule to attract electrons to itself". Over the last 7 decades there have been a number of attempts to quantify this idea and to set up electronegativity scales. It is certainly a success of the whole concept of electronegativity that some of these scales, as for example, those proposed in Refs. [3, 4, 5, 6, 7] correlate fairly well with each other [8], in spite of their varying theoretical and empirical foundations. Given a scale of electronegativity the polarity of a bond is then more or less intuitively connected with the difference in the electronegativity of the bonding partners. However, any attempt to derive quantitative measures of bond polarity from electronegativities poses considerable difficulties. There are a number of formulae relating the "partial ionic character" [4, 9] of bonded atoms to their electronegativity difference [10, 11] but each of them can be criticized for various reasons and, as a consequence, none of them is uniquely accepted today. More importantly, there are intrinsic difficulties when estimating the polarity of a bond between atoms which are linked to further atoms: the number, the geometric arrangement, and the electronegativities of the bonding partners of the atoms under consideration may also influence the polarity of the bond between them. While in many cases these effects may be considered as first- and second-order perturbations of basically atomic electronegativities, this is certainly no longer the case for the metal–metal bonds between transition metals: their nature may be more significantly influenced by the coordination spheres of the metal centers rather than intrinsic properties of the metal itself [12]. In principle, the concept of group electronegativities [8] might provide a way out of these difficulties, but it is an open question whether any of the methods devised so far will give reasonable answers in the aforesaid case.

Instead, it is certainly justified to ask whether the polarity of a bond can be determined directly without reference to atom or group electronegativities. Thirty years ago this point of view was already taken by Klessinger [11], who argued that the one-electron density contains "much more far-reaching information about the polarity of a bond than can be expressed through the values of a couple of parameters from oversimplified models". Here, we adhere to this point of view in that the one-electron density is the key ingredient to the topological definition of "atoms in molecules" (AIM) given by Bader [13, 14] and used here. Yet, it will also be shown

Correspondence to: G. Jansen
e-mail: georg@theochem.uni-duesseldorf.de

that it is possible to condense the information on the polarity of a bond contained in the density into a set of numerical parameters. To do so, one needs both a notion of what an atom in a molecule is and a notion of what is meant by the term bond. In recent years the electron localization function (ELF) [15, 16] has proven to provide a picture of the distribution of core-electron pairs, bonds, lone pairs, etc. which is compatible with many aspects of the traditional Lewis and valence-shell electron-pair repulsion models and at the same time has a sound theoretical foundation in terms of averaged pair densities or, in an alternative interpretation, excess kinetic energies due to the Pauli principle [17, 18, 19]. The pictures of a molecule as drawn by the AIM and ELF analyses are complementary: with AIM the one-electron density of a molecule is composed of fragment electron densities restricted to spatially disjoint "atomic basins", while with a similar partitioning of the three-dimensional space induced by ELF [17, 20, 21] the molecular density is composed of the fragment densities found in spatially disjoint "localization basins" which correspond to those regions of space where core, bond, lone pair or – in open-shell molecules – single electrons tend to localize. Savin et al. [18] have used a combination of both pictures to propose a quantitative definition of the polarity of a bond through the calculation of atomic partial charges using an AIM partitioning of the electron density and the determination of bond populations with an ELF partitioning. If an atom is linked to several atoms, however, all its bonding partners will contribute to its overall partial charge. The determination of the polarity of an individual bond, therefore, seems to be somewhat problematic with this scheme – at least as long as the bonds are not related by symmetry operations.

Another way to combine AIM and ELF partitionings to a topological definition of bond polarity has been proposed by one of us in a study on the polarity of the metal–metal bond in heterobimetallic complexes [12]. It was suggested that the separate integration of the bond population within each atomic domain of the bond partners might provide a strictly quantitative measure of the polarity of a bond. This can be done independently for each of the bonds to a central atom. In the present article we discuss first numerical results on bond polarities obtained from this scheme (Some of the results shown here were presented at the ChemBond workshop, June 1–4, 2000, La Colle-sur-Loup, France [22]). The systems considered here are small linear molecules, for which the required numerical integrations could be carried out with fair accuracy in a short time. Since they serve as the first test of the applicability of our method, they were chosen to be electronically simple molecules for which there are essentially undisputed expectations of their bond polarities. Besides the bond polarities themselves, we also analyze the fluctuations of the underlying basin populations.

The outline of the article is as follows. After an introduction of the necessary theoretical background we give some details of the implementation of the method and the quantum chemical calculations of the molecules considered. After a brief discussion of the core populations we then turn to a detailed discussion of the results for the FCN molecule as an example of a molecule which, according to the traditional picture, should possess a highly polar single bond and a not very polar triple bond. Next we analyze the trend in the bond polarity for the series of hydrogen halides from HF to HBr and discuss the cases of the ionic bond in NaCl and the van der Waals bond in NeAr. We conclude with a summary of the most important findings.

2 Theory

In the theory of AIM an atom (free or bound) is defined as the union of an attractor of the gradient vector field of the one-electron density, $\nabla\rho(\mathbf{r})$, and its associated basin [13, 23]. Most often an attractor of $\nabla\rho(\mathbf{r})$ topologically corresponds to an isolated local maximum or the (3,−3) critical point of the density at the position $\mathbf{r}_a$ of a nucleus. Other, more exotic situations are discussed in Refs. [13, 23]. The atomic basin Ω_a^ρ associated with an attractor consists of the points on all gradient paths which terminate at the attractor. Two neighboring atomic basins Ω_a^ρ and Ω_b^ρ are separated by a surface $S_{ab}^\rho(\mathbf{r})$, called an atomic separatrix, which is never crossed by a gradient path:

$$\nabla\rho(\mathbf{r}) \cdot \mathbf{n}_{ab}^\rho(\mathbf{r}) = 0 \quad \forall\, \mathbf{r} \in S_{ab}^\rho(\mathbf{r}) \ . \tag{1}$$

An atomic separatrix normally contains a (3,−1) or bond critical point (BCP) (for a discussion of exceptional cases containing nonisolated BCPs see Ref. [23]). This can be used to construct the separatrix by following the gradient paths emanating from the BCP in the directions of those two eigenvectors of the associated Hessian matrix which correspond to its negative eigenvalues [24].

In close analogy to the gradient vector field of the one-electron density, the gradient vector field of the electron localization function $\nabla\eta(\mathbf{r})$ can be used to define localization basins Ω_i^η as the union of an attractor of the ELF and the points on all gradient paths which terminate there [17, 21]. In general, the topology of $\eta(\mathbf{r})$ is much more complicated than that of the one-electron density. For linear molecules one regularly finds the occurrence of (2,−2) ring attractors and (2,0) "saddle rings" (Fig. 1). Again, one can use a saddle point or ring in $\eta(\mathbf{r})$ to construct a surface $S_{ij}^\eta(\mathbf{r})$ which is never crossed by a gradient path of the ELF:

$$\nabla\eta(\mathbf{r}) \cdot \mathbf{n}_{ij}^\eta(\mathbf{r}) = 0 \quad \forall\, \mathbf{r} \in S_{ij}^\eta(\mathbf{r}) \ . \tag{2}$$

This surface separates two neighboring localization basins Ω_i^η and Ω_j^η. It is called a localization separatrix in the following. The localization basins themselves may be classified as core basins, $C(X)$, and valence basins [21]. When there are several core basins corresponding to the K, L, and M shells they are denoted as $C_K(X)$, $C_L(X)$, and $C_M(X)$, respectively. The valence basins in our examples will be monosynaptic, $V(X)$, or disynaptic, $V(X,Y)$. X and Y mean the atomic symbol of the nucleus surrounded by the core basins or connected to the valence basins (via core basins), respectively.

Both, the atomic and the localization basins provide a partitioning of three-dimensional space into disjoint

regions. A given localization basin, however, is not necessarily disjoint with a given atomic basin but rather may be completely contained within it or partially overlap with it. This is seen from Fig. 2, which shows a superposition of atomic and localization separatrices for the FCN molecule. The set

$$\Omega_s = \Omega_i^\eta \cap \Omega_a^\rho \tag{3}$$

of the points contained in Ω_i^η and in Ω_a^ρ is called an atomic subbasin of the localization basin and is denoted as $V(X)|Z$ or $V(X,Y)|Z$. Here, Z stands for the atomic symbol of a nucleus contained in the corresponding atomic basin. As indicated by Fig. 2, the core basins, $C(X)$, will usually be completely contained in the corresponding atomic basin, X, while it may happen that a monosynaptic localization basin, $V(X)$, connected to an atomic nucleus X overlaps with the atomic basin containing a second nucleus Y, and similarly a disynaptic localization basin, $V(X,Y)$, with the atomic basin of a third nucleus.

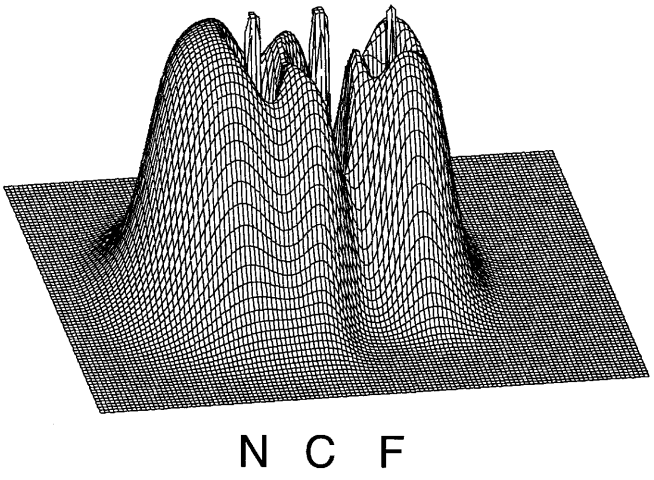

Fig. 1. Relief map of the electron localization function, $\eta(\mathbf{r})$, for the FCN molecule. The cut plane contains the molecular rotation axis. Note that the double maxima behind the F atom and between the C and N atoms become (2,−2) ring-shaped attractors in three dimensions and that the saddle points close to the N, C and F core peaks become (2,0) ring-shaped saddles

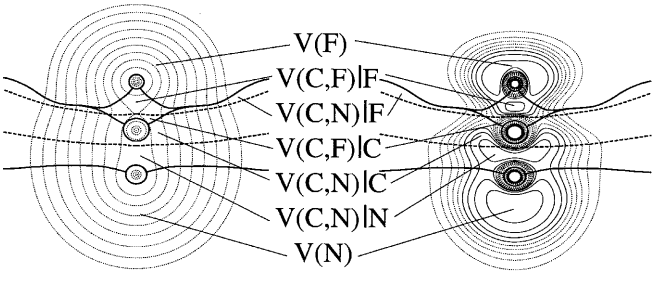

Fig. 2. Superposition of the separatrices between atomic basins (*dashed dark lines*) and localization basins (*solid dark lines*) with contour maps of the density (*left*) and the electron localization function (*right*) for FCN at the B3LYP level. Core basins are not explicitely labeled. The outermost of the contour lines corresponds to values of $\log\rho = -4$ and $\eta = 0.1$; they increase in steps of $\Delta\log\rho = 0.5$ and $\Delta\eta = 0.1$, respectively

The average electron population of a basin is given by

$$\overline{N}_s = \overline{N}(\Omega_s) = \int_{\Omega_s} \rho(\mathbf{r})\mathrm{d}\tau \tag{4}$$

and its variance [13, 21] by

$$\sigma_s^2 = \sigma^2(\overline{N}, \Omega_s) = \int_{\Omega_s}\int_{\Omega_s} \pi(\mathbf{r}_1, \mathbf{r}_2)\mathrm{d}\tau_1\,\mathrm{d}\tau_2 + \overline{N}_s - \overline{N}_s^2 \ , \tag{5}$$

where $\pi(\mathbf{r}_1, \mathbf{r}_2)$ is the spin-summed two-electron density normalized to $N(N-1)$ and N is the total number of electrons [25]. The variance is a measure of the fluctuation of the basin population. It can be broken down into contributions from all other basins [26] as

$$\sigma_s^2 = \sum_{t\neq s} B_{st} \ , \tag{6}$$

where

$$B_{st} = 2\sum_\mu \sum_\nu \int_{\Omega_s} \phi_\mu^*(\mathbf{r})\phi_\nu(\mathbf{r})\mathrm{d}\tau \times \int_{\Omega_t} \phi_\nu^*(\mathbf{r})\phi_\mu(\mathbf{r})\mathrm{d}\tau \tag{7}$$

for a closed-shell Hartree–Fock or Kohn–Sham determinant made up from a set $\{\phi_\mu(\mathbf{r})\}$ of doubly occupied spatial orbitals.

3 Method and technical details

The BCPs used to determine the atomic separatrices were located with a version of the original EXTREME program [24] which was modified to account for f functions. The separatrices were then constructed by following gradient paths in steps of $\ell \cdot \nabla\rho(\mathbf{r})/|\nabla\rho(\mathbf{r})|$, where $\ell = 0.025$ au. For the linear molecules considered here it is sufficient to construct only one such gradient path per BCP in a given plane containing the molecular rotation axis. The initial step away from the BCP could be chosen as small as 0.0001 au in all cases.

Critical points and rings, i.e., (3,−1) and (2,0) saddle points and rings, in the ELF were located with a Newton–Raphson algorithm. To this end, the gradient and the Hessian of the "core-part" D_σ/D_σ^0 of $\eta(\mathbf{r})$ were calculated analytically and implemented in a program which performs automated searches of the critical points and rings in a user-chosen region of space. Localization separatrices were then constructed in a similar way as the atomic separatrices, again using a step length of 0.025 au. Yet, since the topology of $\eta(\mathbf{r})$ may lead to strongly curved separatrices, especially when core basins are involved, the stabilized Euler gradient-path-following algorithm [27, 28] was used. In some cases, the spherical valleys around core basins were so flat that it was impossible to locate (3,−1) and (2,0) saddle points and rings within them. In these cases the entire valley bottom acts as a (1,+1) critical sphere. The separatrix was then obtained as that sphere which minimizes the sum of the ELF values on it. Note that this is an approximation since, for example, the separatrix might be better represented as a distorted ellipsoid. The quality of this approximation was checked by comparing core ba-

sin populations obtained with it to those obtained with separatrices constructed through gradient-path following. For the three core populations of the FCN molecule they agreed to with in about 0.01 electron numbers.

Atomic and localization separatrices were then mapped on a two-dimensional grid with a spatial resolution of 0.005 au. Typical grid sizes ranged from 1200×2400 for the HF molecule to 1500×3400 for NaCl. Each grid point was assigned to a basin employing a recursive algorithm which checks whether the neighboring points have already been assigned to a separatrix or a basin and updates the corresponding information of the point itself accordingly. The numerical integration is then carried out in three steps using cylindrical coordinates. First, for the radial integration of the molecular orbitals and the density an adaptive Clenshaw–Curtis quadrature with a determination of the Chebyshev coefficients through a fast discrete cosine transform [29] was used. Then, for integration in the direction of the molecular rotation axis an ordinary trapezoidal rule with a step length of 0.005 au was employed. Finally, the integrated values were multiplied by 2π for the density and σ orbitals and by π for non-σ orbitals, where degenerate orbital equivalence is enforced for those π and δ orbitals which happen to have a nodal plane in the chosen integration plane.

The total populations obtained with this procedure were accurate to better than 0.005 electron numbers. The accuracy of the individual basin populations depends on the accuracy of the separatrices and the steepness of the density in the basin. On the basis of extensive experimentation with step sizes for the separatrices, map grid sizes, and integration parameters, we estimate it to be of the order of 0.01–0.02 electron numbers for core basins and highly populated valence basins and perhaps better than 0.005 electron numbers for more weakly populated basins.

The molecular orbitals and densities were determined through closed-shell restricted Hartree–Fock (RHF) and density functional theory (DFT) electronic structure calculations with the GAUSSIAN94 program package [30]. In the DFT calculations Becke's three-parameter hybrid functional [31, 32] with the Lee–Yang–Parr correlation potential [33, 34] (B3LYP) was used. All atoms were described with the augmented correlation-consistent polarized valence triple-zeta basis sets of Dunning and coworkers [35, 36, 37, 38], except for the Na atom, which was described with the triple-zeta valence basis set of Schäfer et al. [39] in combination with a (2p1d) polarization function set of Huzinaga [40]. The molecular geometries used in the bond population analysis are given in Table 1. They were obtained from geometry optimizations with the basis sets described previously. In case of the NeAr dimer, however, the geometry is the equilibrium geometry from the empirical $n(r)$-6 class I interaction potential [41].

Table 1. Optimized equilibrium distances (Å) obtained at the restricted Hartree–Fock (*RHF*) level and with Becke's three-parameter hybrid functional with the Lee–Yang–Parr correlation potential (*B3LYP*)

Molecule		RHF	B3LYP
FCN	r_{CN}	1.124	1.151
	r_{FC}	1.243	1.266
HF		0.899	0.924
HCl		1.267	1.283
HBr		1.408	1.425
NaCl		2.394	2.374
NeAr[a]		3.48	3.48

[a] $n(r)$-6 class I potential [41]

4 Results and discussion

The basin populations, their variances, and the percentual contributions of the other basins to the variance of the given basin for the set of molecules considered are displayed in Table 2. In the following we will mainly discuss the B3LYP populations, which contain the effects of electron correlation. Yet, since there are and there will be a large number of increasingly accurate density functional methods Table 2 also contains Hartree–Fock populations for reference. The variance contribution analysis is only given for the B3LYP populations; however, the corresponding results for the Hartree–Fock populations were similar: both agree within a few percent for contributions larger than, say, 10% and mostly within a few tenths of a percent for the smaller contributions.

4.1 Core populations

From Table 2 it is seen that the core populations are nearly independent of the quantum chemical method and, more importantly, of the chemical environment: the RHF and B3LYP results always agree within the estimated numerical accuracy of 0.01–0.02 electron numbers for the core populations, and the core populations of the fluorine atom in FCN and HF and the chlorine atom in HCl and NaCl match within the same limits. Note that the core populations do not exactly agree with chemical expectation. They are somewhat larger than 2 for the K shell, scatter around 8 for the L shell, and the M shell population is somewhat smaller than 18 in the case of the bromine atom. The remaining valence populations of the (hypothetical) free second-row atoms are 3.90 (C), 4.89 (N), 6.86 (F), and 7.83 (Ne), which corresponds to a defect of roughly 0.02 per valence electron compared to the classical integer valence electron numbers. For the third-row atoms there seems to be no simple rule for the defect of the valence electron numbers; here the remaining valence populations are 0.97 (Na), 6.94 (Cl), and 7.95 (Ar). In case of the fourth-row bromine atom one even observes an excess of 0.05 compared to the classical valence population of 7 electron numbers. The actual values for core and valence populations are fully in line with previous findings on atoms and molecules [20, 21, 26].

4.2 FCN

A contour plot of the B3LYP density, the ELF, and the resulting atomic and localization basins for the FCN

Table 2. Average basin electron populations, $\bar{N}_s$, their variances, σ_s^2, and variance contribution analysis (%). The subbasins of V(Cl) found with RHF for NaCl are denoted as *v*(Cl) and *v*(Cl,Na), respectively

Basin	RHF		B3LYP		
	$\bar{N}_s$	σ_s^2	$\bar{N}_s$	σ_s^2	Variance contributions
FCN					
C(N)	2.10	0.28	2.11	0.29	V(N) 49, V(C,N)|N 33, V(C,N)|C 14
V(N)	3.10	1.12	3.31	1.20	V(C,N)|N 46, V(C,N)|C 31 C(N) 12
V(C,N)|N	3.20	1.53	2.63	1.44	V(C,N)|C 44, V(N) 39
V(C,N)|C	1.52	1.20	1.96	1.43	V(C,N)|N 44, V(N) 26, V(F) 10
V(C,N)|F	0.04	0.04	0.05	0.05	V(F) 40, V(C,N)|C 20
C(C)	2.09	0.25	2.10	0.26	V(C,N)|C 38, V(C,N)|N 23, V(N) 13
V(C,F)|C	0.21	0.20	0.23	0.22	V(F) 32, V(C,F)|F 22, V(C,N)|C 16
V(C,F)|F	1.15	0.77	0.97	0.69	V(F) 68, V(C,N)|C 12, V(C,F)|C 7
V(F)	6.45	1.12	6.50	1.15	V(C,F)|F 41, C(F) 28, V(C,N)|C 12
C(F)	2.14	0.36	2.14	0.37	V(F) 87, V(C,F)|F 8
HF					
C(F)	2.13	0.36	2.14	0.37	V(F) 86, V(F,H)|F 11
V(F)	6.40	1.03	6.47	1.03	V(F,H)|F 57, C(F) 31, V(F,H)|H 12
V(F,H)|F	1.25	0.77	1.12	0.73	V(F) 80, V(F,H)|H 14, C(F) 6
V(F,H)|H	0.22	0.19	0.27	0.24	V(F) 53, V(F,H)|F 43, C(F) 4
HCl					
C_K(Cl)	2.18	0.54	2.18	0.54	C_L(Cl) 96, V(Cl) 3
C_L(Cl)	7.89	1.03	7.88	1.05	C_K(Cl) 49, V(Cl) 43, V(Cl,H)|Cl 5
V(Cl)	6.14	1.13	6.24	1.15	C_L(Cl) 39, V(Cl,H)|Cl 36, V(Cl,H)|H 23
V(Cl,H)|Cl	1.09	0.76	0.97	0.70	V(Cl) 60, V(Cl,H)|H 32, C_L(Cl) 8
V(Cl,H)|H	0.70	0.49	0.73	0.50	V(Cl) 51, V(Cl,H)|Cl 44, C_L(Cl) 5
HBr					
C_K(Br)	2.18	0.63	2.19	0.63	C_L(Br) 92, C_M(Br) 8
C_L(Br)	8.52	1.85	8.51	1.85	C_M(Br) 66, C_K(Br) 31
C_M(Br)	17.25	2.15	17.25	2.19	C_L(Br) 56, V(Br) 35, V(Br,H)|Br 5
V(Br)	6.21	1.39	6.31	1.44	C_M(Br) 54, V(Br,H)|Br 22, V(Br,H)|H 21
V(Br,H)|Br	0.92	0.70	0.84	0.65	V(Br) 49, V(Br,H)|H 33, C_M(Br) 17
V(Br,H)|H	0.92	0.56	0.90	0.56	V(Br) 53, V(Br,H)|Br 38, C_M(Br) 8
NaCl					
C_K(Cl)	2.18	0.54	2.18	0.54	C_L(Cl) 96, V(Cl)|Cl 4
C_L(Cl)	7.88	1.03	7.87	1.05	V(Cl)|Cl 50, C_K(Cl) 49
V(Cl)|Cl	7.86	0.63	7.84	0.69	C_L(Cl) 77, C_L(Na) 12, V(Cl)|Na 8
v(Cl)|Cl	6.44	1.23			
v(Cl,Na)|Cl	1.42	0.88			
V(Cl)|Na	0.05	0.05	0.08	0.08	V(Cl)|Cl 67, C_L(Na) 29
v(Cl)|Na	0.01	0.01			
v(Cl,Na)|Na	0.04	0.04			
C_L(Na)	7.85	0.52	7.86	0.54	C_K(Na) 80, V(Cl)|Cl 15, V(Cl)|Na 4
C_K(Na)	2.18	0.44	2.17	0.44	C_L(Na) 100
NeAr					
C_K(Ar)	2.19	0.55	2.19	0.55	C_L(Ar) 95, V(Ar) 5
C_L(Ar)	7.87	1.08	7.86	1.09	V(Ar) 52, C_K(Ar) 48
V(Ar)	7.94	0.58	7.95	0.61	C_L(Ar) 94, C_K(Ar) 4, V(Ne) 1
V(Ne)	7.83	0.41	7.83	0.42	C(Ne) 98, V(Ar) 2
C(Ne)	2.17	0.40	2.17	0.41	V(Ne) 100

molecule in a plane containing the molecular rotation axis is shown in Fig. 2. A plot of the corresponding RHF quantities is not shown since it was virtually indistinguishable for the eye. On the right-hand side of the figure one can clearly see a toruslike structure slightly above the fluorine nucleus which corresponds to the region occupied by three lone pairs in sp^3 orbitals of the classical hybrid orbital model. Yet, the population of the monosynaptic valence basin V(F) is found to be 8% larger than the idealized value of 6. Viewing this from a different perspective, one can also say that 95% of the average 6.86 valence electrons of the free fluorine atom (Sect. 4.1) will find themselves localized in the monosynaptic basin V(F) after binding to the C–N fragment. The fluorine atom invests only an average of 0.36 electrons into the bond with the carbon atom. The remaining 0.84 electrons to the overall population of 1.20 electron numbers for the V(C,F) disynaptic basin (Table 3) come from the carbon atom, and most of that contribution is transferred to the atomic basin of the fluorine atom, thus yielding the main contribution to the partial charge of −0.66 elementary charges on the fluorine atom. Table 3, which summarizes partial atomic charges, q_a, total disynaptic basin populations,

Table 3. Partial charges, q_a (in elementary charges), average electron populations of the disynaptic basins, $\bar{N}[V(X,Y)]$, and percentual atomic contributions, a_a, to $\bar{N}[V(X,Y)]$ as obtained with the B3LYP functional

	q_a	$\bar{N}[V(X,Y)]$	a_a	$\bar{N}[V(Y,Z)]$	a_a
FCN					
N	−1.05	4.64	57		
C	1.71		42	1.20	19
F	−0.66		1		81
HF					
F	−0.73	1.39	81		
H	0.73		19		
HCl					
Cl	−0.27	1.70	57		
H	0.27		43		
HBr					
Br	−0.10	1.74	48		
H	0.10		52		
NaCl					
Cl	−0.89	7.92[a]	99		
Na	0.89		1		

[a] $\bar{N}[V(X)]$

and their percentual atomic contributions, a_a, demonstrates that 81% of the V(C,F) basin population is localized in the fluorine atomic basin – a result which agrees very well with the expectation of the C–F bond polarity on the basis of electronegativity arguments. Furthermore, from Fig. 2 and Table 2 it is seen that even a small fraction of 0.05 electron numbers of $\overline{N}[V(C,N)]$ is pulled over into the fluorine atomic basin, which again may be rationalized with the strong electronegativity of the fluorine atom in combination with the relative diffuseness of the electron distribution in the C–N bond region. The average V(C,N) basin population of 4.64 electrons itself is only weakly polarized: 57% of it is localized in the atomic domain of the more strongly electronegative nitrogen atom. Since test calculations on a free cyanide ion gave a much more strongly polarized disynaptic basin population with 83% nitrogen contribution, one may argue that the electron-pulling effect of the fluorine atom indirectly leads to a depolarization of the C–N bond. Despite that, the nitrogen atom bears a strong partial charge of −1.05 elementary charges. One may regard the excess electron as being localized in the monosynaptic V(N) basin, whose average electron number is 3.31. On the basis of the classical Lewis structure and the localized orbital model one would interprete the V(N) basin as the basin of a single lone pair in an sp^1 orbital with an idealized occupation number of 2. Thus, reinterpreting the much larger average electron number calculated for V(N) in classical terms one is led to postulate the contribution of an "ionic" resonance structure to the electronic structure, in which the nitrogen atom has two lone pairs and is doubly bound to the carbon atom. The total electronic structure would then be a mixture of this ionic structure, the usual Lewis structure with a single lone pair and a triple bond, and a truly ionic structure NC^+F^-.

This interpretation is supported by the values for the variance, σ^2, of the V(N) and V(C,N) basins and the variance contribution analysis given in Table 2. The variance of 1.20 for the V(N) basin and that of 1.62 for the combined V(C,N) basin (not given in the table) are not small compared to the basin populations. The relative fluctuations, $\lambda = \sigma^2/\overline{N}$, [21, 26] amount to 0.36 for the V(N) and 0.35 for the V(C,N) basin populations, respectively. 77% of the fluctuation of the V(N) basin population is due to that of V(C,N) and, vice versa, 58% of the variance of the latter is due to the former, thus indicating a noticeable delocalization of the electrons between the two basins. In contrast, the relative fluctuations of the core basins and that of the V(F) basin are all below 0.18, indicating a much higher degree of localization in these basins. The population of the V(C,F) basin has a variance of 0.81 (not given in the table) and, owing to its small average electron number of only 1.20, a large relative fluctuation of 0.68. The main contributor to this fluctuation is the V(F) basin population (67%), another 20% comes from the C–N bond population.

On splitting the V(C,N) basin into atomic contributions, the variances of the resulting V(C,N)|N and V(C,N)|C subbasins drop by only about 0.2 from the variance of 1.62 found for the whole basin (Table 2). As a consequence, the relative fluctuations, λ, reach values of 0.55 for V(C,N)|N and of 0.73 for V(C,N)|C, respectively, while for the third and only very weakly populated V(C,N)|F subbasin λ attains its limiting value of 1. It appears to be natural that the most important contributors to the fluctuation in the population of a given atomic subbasin of a bond electron pair localization basin should be the other atomic subbasins of the same localization basin. Table 2 shows that this expectation is fulfilled for V(C,N)|N and V(C,N)|C: each of them represents with a 44% contribution to the variance in the electron population of the respective other basin the most important partner for interbasin fluctuation of electrons. Yet, from the table it also becomes clear that a simple percentual variance contribution analysis may be misleading in this respect. In the case of the V(C,F) basin, the population of V(F) is still the most important contributor to the fluctuation of both, $\overline{N}[V(C,F)|C]$ and $\overline{N}[V(C,F)|F]$, and the population of V(C,N)|C contributes even more to the fluctuation of $\overline{N}[V(C,F)|F]$ than does the population of V(C,F)|C. This can simply be explained by the comparatively small average electron populations of the atomic subbasins of V(C,F). Taking into account that $\overline{N}[V(F)]$ is 28 times and $\overline{N}[V(C,N)|C]$ still more than 8 times larger than $\overline{N}[V(C,F)|C]$ it is evident that the electrons in V(C,F)|F exchange much more easily with those in V(C,F)|C rather than with the electrons in V(F) or in V(C,N)|C. Weighting the variance contributions to the atomic subbasin populations of V(C,N) in the same way underlines their reciprocal predominant role for the exchange of electron population, though V(N) remains an important partner for the fluctuation between its electrons and those of V(C,N)|N and V(C,N)|C.

To summarize the most essential findings of this subsection it is convenient to introduce a simplified language which resembles the traditional notions of the

order and the partial ionic character of a bond but replaces them with precisely defined terms calculated from the combined ELF/AIM analysis presented here. For a two-center bond the average bond electron pair number is given as

$$b_{XY} = \overline{N}[V(X,Y)]/2 \ .$$

This term, which is defined from the ELF analysis alone, has already been used implicitly as a substitute for the bond order [21, 42]. The combined ELF/AIM analysis now allows the introduction of a bond polarity index as

$$p_{XY} = \frac{a_X - a_Y}{100} = \frac{\overline{N}[V(X,Y)|X] - \overline{N}[V(X,Y)|Y]}{\overline{N}[V(X,Y)|X] + \overline{N}[V(X,Y)|Y]} \ ,$$

where a_X should be the larger of the percentual atomic contributions. This index ranges between 0 for homopolar bonds and 1 for idealized ionic bonds, where one of the a_a will be 0. It shares this convenient property with Pauling's original definition of the partial ionic character of a bond via an exponential function of the square of the electronegativity difference [4] and, very recently, a similar definition has also been advocated by Bernard Silvi. Using b_{XY} and p_{XY}, we may say that the F–C bond in FCN has the character of a partial single bond formed by an average of 0.60 bond electron pairs which are strongly polarized towards the F atom with a polarity of 0.62. The C–N bond is a double-to-triple bond formed by 2.32 bond electron pairs which are weakly polarized towards the N atom with a polarity of 0.15. Furthermore, there is a marked resonance fluctuation between the C–N bond and the nitrogen lone-pair electron populations.

This picture is somewhat different when using the Hartree–Fock wavefunction: here the average bond electron pair number of the F–C bond is 0.68 and its polarity 0.70, while 2.38 electron pairs with a polarity of 0.33 form the C–N bond. The marked overestimation of the C–N bond polarity together with the slight overestimation of the bond population leads to a strongly increased negative charge attributed to the nitrogen atom which is partially compensated by a reduced V(N) population (Table 2) to yield a total partial charge of -1.40 elementary charges. This is a significant overestimation compared to the value of -1.05 found with the B3LYP density. Similarly, the somewhat too large partial charge of -0.78 elementary charges found for the fluorine atom is caused by the combined effect of slightly overestimated C–F bond population and polarity. Nevertheless, it is gratifying to see that qualitatively there is not much difference between the analyses of the bonds in FCN at the Hartree–Fock and the B3LYP levels of theory.

4.3 Hydrogen halides

The contour plot of the density, the ELF, and the atomic and localization basins of the hydrogen chloride molecule shown in Fig. 3 is representative for the three hydrogen halides considered here, the obvious difference being the number of core basins. For HCl and HBr the

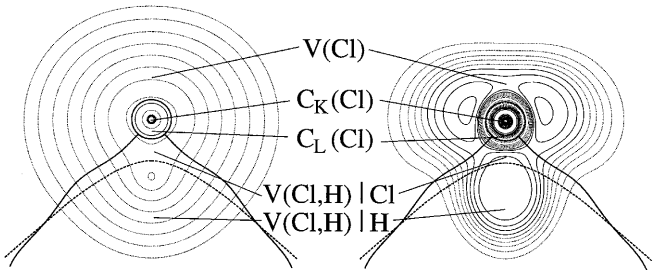

Fig. 3. As in Fig. 1 for HCl

localization separatrix crosses the atomic separatrix at density values smaller than $2 \times 10^{-3.5}$ au, while for HF such a crossing was not observed. As a consequence, the populations of what would have to be classified as V(X)|H basins were found to be negligible, i.e., below 3×10^{-4} electron numbers, and were left out of Table 2.

As in the case of the fluorine atom in FCN, in the contour plot of $\eta(\mathbf{r})$ for HCl and the other hydrogen halides one can identify a toruslike structure slightly above the halogen nucleus which corresponds to the three lone pairs in sp^3 orbitals of the traditional orbital model. Again, for all the hydrogen halides the populations of the V(X) basin are larger than the idealized value of 6 (by 4–8%). Note that $\overline{N}$[V(F)] in HF is only very slightly different from $\overline{N}$[V(F)] in FCN as may be expected for such a "hard" element. Comparing the populations of the monosynaptic V(X) basin to the valence populations of the free halogen atoms (Sect. 4.1) one finds that the fluorine atom invests only 0.39 electrons into the bond with the hydrogen atom, the chlorine atom 0.70, and the bromine atom 0.74. Owing to its missing core the hydrogen atom always has to give its electron into the bond, thus yielding total disynaptic basin populations of 1.39, 1.70, and 1.74, respectively. As demonstrated in Table 3, in the case of HF 81% of $\overline{N}$[V(F, H)] is localized in the V(X,H)|X subbasin, while for the other hydrogen halides the bond population is shared in approximately equal portions between the atoms.

Looking at the percentual variance contributions found in Table 2 one notes that in each case for both the V(X,H)|X and V(X,H)|H subbasins the V(X) basin is the most important partner for fluctuation between the electron populations – as was similarly observed for the subbasins of V(C,F) in FCN. Taking into account that in every case $\overline{N}$[V(X)] is at least 6 times larger than $\overline{N}[V(X,H)|X]$ or $\overline{N}[V(X,H)|H)]$ it becomes clear that nevertheless the electrons fluctuate much more easily between the two subbasins of V(X,H) than with V(X). Still, there is a noticeable resonance fluctuation between the bond and the lone-pair electron populations: the variances $\sigma^2[\overline{N}, V(X,H)]$, of the populations of the entire V(X,H) basins (not given in Table 2) are 0.76, 0.76, and 0.78 for HF, HCl, and HBr, respectively. These values correspond to large relative fluctuations between 0.45 and 0.55 and they are to 80% and more due to the population of V(X).

The average bond electron pair number, b_{XH}, increases from 0.70 to 0.85 to 0.87 in the series HF, HCl,

and HBr, while at the same time the polarity, $p_{X\mathrm{H}}$, decreases from 0.62 to 0.14 to 0.04. In contrast to the situation for HF and HCl, the last value for HBr corresponds to a very slight polarization of the bond charge distribution in the direction of the hydrogen atom. The trend in $p_{X\mathrm{H}}$ agrees fairly well, but not exactly, with what could be expected from electronegativity arguments. The ionic characters of the *X*–H bond as given by Pauling, for example, decrease from 0.60 to 0.19 to 0.11 along the same series [4], where, however, the bond charge distribution is supposed to be always polarized in the direction of the more electronegative halogen atom. Yet, one should note that even though the H–Br bond is found to be practically homopolar with the ELF/AIM analysis there is a noticeable negative partial charge of −0.10 elementary charges on the bromine atom. The explanation for this seeming contradiction is that the average number of bond electron pairs is smaller than 1, so the hydrogen atom necessarily becomes positively charged. This very nicely demonstrates that even for diatomic molecules there is no direct correlation between bond polarities and atomic partial charges and that the number of bond electrons plays an essential role as well – a fact which seems to have gone unnoticed in many discussions.

On the Hartree–Fock level $b_{X\mathrm{H}}$ is slightly larger for all three examples: it increases from 0.74 to 0.90 to 0.92 in the series HF, HCl, and HBr. The polarities of 0.70 and 0.22 for HF and HCl are also slightly larger than their B3LYP counterparts, while the HBr bond is found to be exactly homopolar.

4.4 NaCl

The electron localization function of NaCl as calculated from the B3LYP determinant reveals no sign of a bond electron pair and correspondingly there is no disynaptic V(Cl,Na) basin to be seen on the right-hand side of Fig. 4. Instead there is only one deformed sphere of high η values around the two core shells of chlorine giving rise to a monosynaptic V(Cl) basin. Classically this basin corresponds to the region occupied by the four valence electron pairs of a chloride anion. The average population, $\overline{N}[\mathrm{V(Cl)}]$ is found to be 7.92 electron numbers, which is almost exactly one electron more than the valence population of 6.94 for the neutral free chlorine atom (Sect. 4.1). These findings clearly indicate a purely ionic electronic structure for the sodium chloride molecule. Note that the localization separatrix surrounding $\mathrm{C_L(Na)}$ is strongly deformed from a spherical shape and that the shape of this deformation indicates that the electrons localized in the L shell of Na are repelled from the valence charge distribution of the chloride ion which, on the other hand, is seen to be polarized towards the sodium ion. The atomic separatrix is nicely located in the valley of $\eta(\mathbf{r})$ found between the outermost regions of high η values around the sodium and chlorine nuclei, so only a very small part of the average population of V(Cl) is located in the atomic basin of sodium: $\overline{N}[\mathrm{V(Cl)|Na}]$ is only 0.08 electron numbers or 1% of the total $\overline{N}[\mathrm{V(Cl)}]$ (Tables 2, 3).

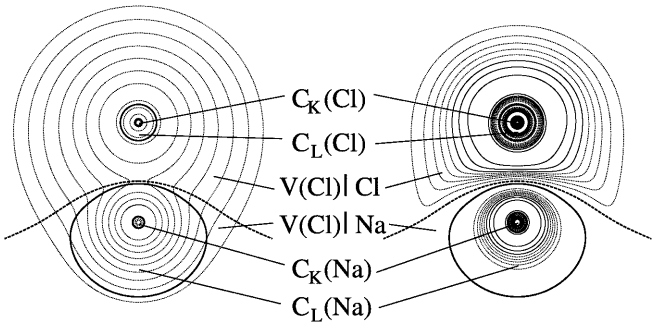

Fig. 4. As in Fig. 1 for NaCl

Nevertheless, this small part of the average population of V(Cl) which is located in the sodium atomic basin is mainly responsible for the fact that the positive charge of the sodium ion in NaCl is 11% smaller than the idealized value of +1.

While there was no sign of a disynaptic V(Cl,Na) basin when calculating $\eta(\mathbf{r})$ with the B3LYP functional, in the Hartree–Fock case our algorithm did detect a (2,0) saddle ring in the outermost sphere of high η values around the chlorine nucleus. This unexpected finding could be verified by optical inspection of the corresponding region at very high resolution. The saddle ring could be used as the starting point for the construction of a localization separatrix between two subbasins called v(Cl) and v(Cl,Na) of what was only one V(Cl) basin at the B3LYP level. These basins, in turn, are further subdivided by the atomic separatrix. As shown in Table 2, only a small part of 0.04 electron numbers of $\overline{N}[v(\mathrm{Cl,Na})]$ is located in the sodium atomic basin. As a consequence, the polarity of the formal bond electron pair population is 0.95, which also suggests the classification of the bond in sodium chloride as purely ionic – independent of the theoretical approximation of its electronic structure.

4.5 NeAr

Looking at the contour maps of $\rho(\mathbf{r})$ and $\eta(\mathbf{r})$ and the corresponding basins for the NeAr dimer shown in Fig. 5 the most important observation is that the localization separatrix between V(Ne) and V(Ar) closely follows the atomic separatrix. The small basin called Δ which is located between the two separatrices was found to contain only about 0.001 electrons on average – a number which is of the same order of magnitude as our estimated numerical accuracy for very weakly populated basins. From the average electron populations given in Table 2 it is seen that the net charges on the atoms are zero within numerical accuracy.

The close resemblance between the atomic and the valence localization basin separatrices is exactly what one would hope to find for a chemically nonbonded dimer. Note that the shape of $\eta(\mathbf{r})$ indicates a repulsion between the valence electrons of neon and argon. This is completely in line with the purely repulsive behavior of the interaction potential-energy curve on the Hartree–

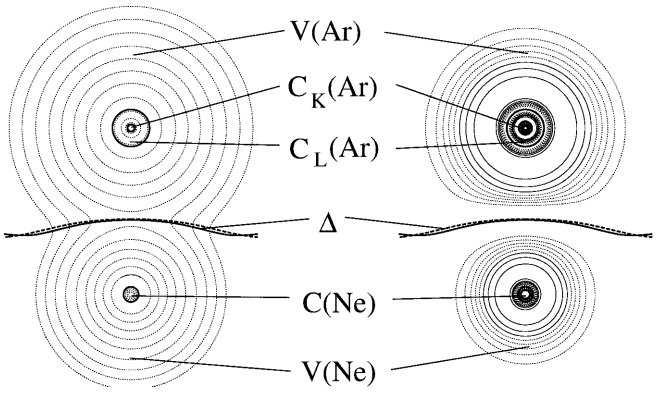

Fig. 5. As in Fig. 1 for NeAr

Fock level, which becomes attractive only owing to intermonomer correlation effects, i.e., dispersion forces. Furthermore, the variance contribution analysis given in Table 2 demonstrates that the valence electron population of one atom hardly contributes to the fluctuation in the valence electron population of the other atom, namely by 2% and less. Clearly the electrons of an atom remain very well localized within their own atomic basin upon dimerization, as expected for a system without a chemical bond.

5 Summary and conclusions

In this study we have presented the first numerical results obtained with a recently proposed quantitative measure for the polarity of a bond [12] through the electron populations of the disjoint atomic subbasins $\Omega_s = \Omega_i^\eta \cap \Omega_a^\rho$ of a bond electron localization basin Ω_i^η. Both Ω_i^η and the atomic basins Ω_a^ρ derive from an analysis of the topology of simple spatial functions, the ELF, $\eta(\mathbf{r})$, on the one hand, and the electronic density, $\rho(\mathbf{r})$, as the key ingredient of the AIM theory on the other. The bond polarity index from the combined ELF/AIM scheme as defined here refers to a localized spatial picture of the bond. Additional information on the fluctuation of the electrons between the various basins and subbasins and, thus, on the amount of delocalization can be obtained from investigation of the variance of the basin populations, as has been shown before for the separate AIM [13] and ELF [21, 26] analyses. After an appropriate weighting with the average electron numbers of the subbasins involved such a variance contribution analysis shows that the electron population fluctuates much more easily between the atomic subbasins of a common bond localization basin than with other bond, lone pair, or core localization basins – as should be expected.

In order to test our method it was applied to a number of molecules with very simple and well-characterized electronic structures. In agreement with common expectation it was found that there is no (chemical) bond between the atoms in the NeAr van der Waals dimer, that the bond in NaCl is purely ionic, and that the polarity of the *X*–H bond decreases in the series HF, HCl, and HBr. One may consider it as a slight surprise that the bond in HBr was found to be nearly exactly homopolar although there is a noticeable partial charge of 0.1 electron numbers on the hydrogen atom. Yet, this is a natural consequence of an average number of bond electron pairs somewhat smaller than 1. In general, in any nonsymmetrical bonding situation partial atomic charges may simply result from noninteger bond electron pair numbers without implying that the bond itself be heteropolar.

The FCN molecule was investigated as an example with a slightly more complicated electronic structure. The ELF/AIM analysis yields perfectly reasonable results in this case as well: the F–C bond has a bond electron pair number of 0.60 and is strongly polarized towards the fluorine atom with a bond polarity index of 0.62, while 2.32 electron pairs, which are weakly polarized towards the nitrogen atom with a polarity of 0.15 form, the C–N bond. These results, the partial charges on the atoms, and the variance contribution analysis are compatible with a resonance picture containing the usual Lewis structure with the F–C bond as a single bond and the C–N bond as a triple bond, an ionic structure NC^+F^-, and a further "ionic" structure with a double bond between C and N and two lone pairs at the nitrogen atom.

Clearly, though the results of the present study are very encouraging the number of test molecules should be significantly enlarged in order to study the performance of the ELF/AIM bond polarity index in the analysis and prediction of trends along the periodic table. Furthermore, other more complicated bonding situations need to be considered, and a three-dimensional integration algorithm is required to study nonlinear molecules. In this laboratory and elsewhere work along these lines is underway.

References

1. Huheey JE, Keiter EA, Keiter RL (1993) Inorganic chemistry: principles of structure and reactivity, 4th edn. HarperCollins, New York
2. Atkins PW, Jones L (1999) Chemical principles: the quest for insight. Freeman, New York
3. Pauling L (1932) J Am Chem Soc 54: 3570
4. Pauling L (1960) The nature of the chemical bond, 3rd edn. Cornell University Press, Ithaca, NY
5. Mulliken RS (1934) J Chem Phys 2: 782
6. Allred AL, Rochow EG (1958) J Inorg Nucl Chem 5: 264
7. Allen LC (1989) J Am Chem Soc 111: 9003
8. Mullay J (1987) Struct Bond 66: 1
9. Pauling L (1931) J Am Chem Soc 53: 1367
10. Hinze J (1968) Fortschr Chem Forsch 9: 448
11. Klessinger M (1970) Angew Chem 82: 534
12. Jansen G, Schubart M, Findeis B, Gade LH, Scowen IJ, McPartlin M (1998) J Am Chem Soc 120: 7239
13. Bader RFW (1990) Atoms in molecules. Oxford University Press, Oxford
14. Bader RFW (1991) Chem Rev 91: 893
15. Becke AD, Edgecombe KE (1990) J Chem Phys 92: 5397
16. Savin A, Becke AD, Flad J, Nesper R, Preuss H, von Schnering HG (1991) Angew Chem Int Ed Engl 30: 409
17. Silvi B, Savin A (1994) Nature 371: 683
18. Savin A, Nesper R, Wengert S, Fässler TF (1997) Angew Chem Int Ed Engl 36: 1809

19. Fässler TF, Savin A (1997) Chemie Unserer Zeit 31: 110
20. Kohout M, Savin A (1996) Int J Quantum Chem 60: 875
21. Savin A, Silvi B, Colonna F (1996) Can J Chem 74: 1088
22. Theor Chem Acc (2001) Volume 105, issue 4–5
23. Bader RFW, Nguyen-Dang TT, Tal Y (1981) Rep Prog Phys 44: 893
24. Biegler-König FW, Bader RFW, Tang TH (1982) J Comput Chem 3: 317
25. McWeeny R (1992) Methods of molecular quantum mechanics, 2nd edn. Academic, London
26. Noury S, Colonna F, Savin A, Silvi B (1998) J Mol Struct (THEOCHEM) 450: 59
27. Ishida K, Morokuma K, Komornicki A (1977) J Chem Phys 66: 2153
28. Schlegel HB (1995) In: Yarkony DR (ed) Modern electronic structure theory, part I. World Scientific, Singapore, p 459
29. Press WH, Teukolsky SA, Vetterling WT, Flannery BP (1992) Numerical recipes in C, 2nd edn. Cambridge University Press, Cambridge
30. Frisch MJ, Trucks GW, Schlegel HB, Gill PMW, Johnson BG, Robb MA, Cheeseman JR, Keith T, Petersson GA, Montgomery JA, Raghavachari K, Al-Laham MA, Zakrzewski VG, Ortiz JV, Foresman JB, Cioslowskii J, Stefanov BB, Nanayakkara A, Challacombe M, Peng CY, Ayala PY, Chen W, Wong MW, Andres JL, Replogle ES, Gomperts R, Martin RL, Fox DJ, Binkley JS, Defrees DJ, Baker J, Stewart JJP, Head-Gordon M, Gonzalez C, Pople JA (1995) Gaussian94, revision E2. Gaussian, Pittsburgh, Pa
31. Becke AD (1993) J Chem Phys 98: 5648
32. Barone V (1994) Chem Phys Lett 226: 392
33. Lee C, Yang W, Parr RG (1988) Phys Rev B 37: 785
34. Miehlich B, Savin A, Stoll H, Preuss H (1989) Chem Phys Lett 157: 200
35. Dunning TH Jr (1989) J Chem Phys 90: 1007
36. Kendall RA, Dunning TH Jr, Harrison RJ (1992) J Chem Phys 96: 6796
37. Woon DE, Dunning TH Jr (1993) J Chem Phys 98: 1358
38. Woon DE, Dunning TH Jr (1994) J Chem Phys 100: 2975
39. Schäfer A, Huber C, Ahlrichs R (1994) J Chem Phys 100: 5829
40. Huzinaga S (ed) (1984) Gaussian basis sets for molecular calculations. Physical sciences data 16, Elsevier, Amsterdam, pp 23, 25
41. Maitland GC, Rigby M, Smith EB, Wakeham WA (1981) Intermolecular forces. Oxford University Press, Oxford, p 582
42. Llusar R, Beltrn A, Andrés J, Noury S, Silvi B (1999) J Comput Chem 20: 1517